Available online at www.sciencedirect.com
SCIENCE DIRECT®
Talanta 67 (2005) 498–502
Talanta
www.elsevier.com/locate/talanta

Fabrication and optical characterization of imaging fiber-based nanoarrays

Jenny M. Tam [1], Linan Song [1], David R. Walt *

Department of Chemistry, Tufts University, Medford, MA 02155, USA

Available online 27 July 2005

Abstract

In this paper, we present a technique for fabricating arrays containing a density at least 90 times higher than previously published. Specifically, we discuss the fabrication of two imaging fiber-based nanoarrays, one with 700 nm features, another with 300 nm features. With arrays containing up to 4.5×10^6 array elements/mm^2, these nanoarrays have an ultra-high packing density. A straightforward etching protocol is used to create nanowells into which beads can be deposited. These beads comprise the sensing elements of the nanoarray. Deposition of the nanobeads into the nanowells using two techniques is described. The surface characteristics of the etched arrays are examined with atomic force microscopy and scanning electron microscopy. Fluorescence microscopy was used to observe the arrays. The 300 nm array features and the 500 nm center-to-center distance approach the minimum feature sizes viewable using conventional light microscopy.

Keywords: Nanoarray; Nanosphere; Imaging fiber bundle; Fiber optic

1. Introduction

As high-throughput techniques, such as gene target screening and genomics mapping increase their dependence on array-based technologies, there is a need for higher density arrays. Although microarray technology has proven to be a valuable tool for many biological applications [1–4], the rapid pace of new gene and protein discovery will necessitate a drive to further miniaturize these platforms in order to offer higher densities, greater sensitivities, and reduced sample volume. To meet these requirements, array elements must shrink from the micron to the nanometer scale.

Nanosensor arrays have been fabricated previously using several methods including dip-pen nanolithography [5–7], ink-jet spotting techniques [8], photolithography [9], and thin film immobilization [10] on polymer wafers. While some of these fabrication methods approach nanoscale feature sizes, several are serial in nature and others produce nanoscale features only in a single dimension and remain microscale in other dimensions.

Optical imaging fiber bundles offer a unique platform for microarray-based techniques. Optical fiber microarrays are fabricated by preferentially etching the fiber cores relative to the cladding, thereby creating wells on the face of the bundle. Beads are then loaded into the wells by self-assembly methods [11,12]. Because of their precise, spatially defined arrangement and their highly parallel format, optical fiber bundles are ideal for array-based applications, such as vapor detection [11,13–15], genomics analysis [12,16–18], and immunoassays [19]. Single nano-optical fibers have been used for fabricating nanoscale devices [20–24] and for sensing and monitoring cellular analytes [25].

Our laboratory has previously fabricated nanoarrays [26] by employing a pipette puller to decrease the array size. While effective, these pulled arrays were difficult to polish, as the overall diameter of the array was too small to handle easily. In this paper, we report a simple, two-step polishing and etching technique that provides two ultra-high density arrays comprised of nanowells with core sizes of 700 and 300 nm. The array elements detailed here are several orders of magnitude smaller than those in conventional arrays

* Corresponding author. Tel.: +1 617 6273470; fax: +1 617 6273443.
E-mail address: david.walt@tufts.edu (D.R. Walt).
[1] Both authors contributed equally to this work.

0039-9140/$ – see front matter © 2005 Elsevier B.V. All rights reserved.
doi:10.1016/j.talanta.2005.06.021

[27]. The high packing density of the array elements is advantageous for high-throughput screening applications. In addition, the packing density provides the ability to include many replicates of all array elements, resulting in a high signal-to-noise ratio by summing signals from the replicates. The high density of nanosensors (4.5×10^6 sensors/mm^2) on the array is at least 90 times higher than other conventional array-based techniques.

2. Experimental

2.1. Fiber bundle preparation

Two types of imaging fiber bundles were obtained from Schott Fiber Optics (Southbridge, MA): fibers with 700 nm cores (1 μm center-to-center spacing) and with 300 nm cores (500 nm center-to-center spacing). These fiber bundles were polished on an Ultra Tec Ultra Pol fiber polisher (Santa Ana, CA) with a series of lapping films using successively finer grit sizes (Mark V Laboratories, East Granby, CT): 20, 12, 9, 3, 1, and 0.1 μm. The fibers were rinsed with nanopure water from a Millipore Milli-Q A10 Synthesis Nanopure water system (Billerica, MA) during the polishing procedure. Between each lapping film, the fibers were sonicated (Cole Parmer, Vernon Hills, IL) for 5 min in nanopure water to remove any residual grit from the fiber surface.

2.2. Etching the fiber bundle to create the nanoarray

Fiber bundles were etched by immersion in a solution of 1 mM HCl. The nanofibers with 700 nm cores were etched for 75 s, and the nanofibers with 300 nm cores were etched for 40 s. The solution was stirred with a micro-stir bar during the etching process to promote uniform etching. The nanoarrays were rinsed with nanopure water for 60 s to stop the etching process and were then sonicated for 20 s to remove any residual salts from the array surface.

2.3. Nanoarray preparation

Rhodamine B-dyed polystyrene 700 and melamine 300 nm beads were obtained from microParticles GmbH (Berlin, Germany) and Bangs Laboratories (Fishers, IN). A solution of each nanobead type was created by making a 1:100 dilution of concentrated bead stock in nanopure water. An array of nanobeads was created using two methods: (1) depositing an aliquot of nanobead solution onto the etched face of the fiber bundle; and (2) loading dried beads onto the array by mechanical force.

In the first approach, a 0.2 μL aliquot of nanobead solution was placed on the etched end of the fiber bundle, and the nanobeads localized into the complementary-sized nanowells as the solution evaporated. Using a higher concentration of the nanobead solution or adding more than one aliquot of solution onto the fiber achieved higher density loading. The fiber surface was cleaned by softly swabbing the surface with a cleanroom swab moistened with nanopure water in order to remove any aggregated beads.

In the second method, a high packing density of nanobeads was created by force loading dried beads into the nanoarray. A highly concentrated nanobead solution was filtered and then dried in an oven at 60 °C for 2 h. The beads were then deposited by lightly tapping the etched fiber face into the nanobead powder. The beads were then cleaned gently by wiping the surface with a cleanroom swab.

2.4. Instrumentation

Tapping-mode atomic force microscopy with a Digital Instruments Dimension 3000 atomic force microscope (Veeco Metrology, Santa Barbara, CA) was used to analyze fiber topology. High-aspect ratio tips (FIB2-100) from Veeco Probes (Santa Barbara, CA) were used to analyze the nanowell shape and depth and to minimize tip effects from the sidewalls of the nanowells.

A field emission scanning electron microscope (FE-SEM) (LEO 982, Carl Zeiss SMT, Thornwood, NY) was also used to analyze the surface and size dimensions of the nanoarray. This FE-SEM visualized the nanoarray using low accelerating voltages (1 keV), minimizing charging effects of the silica without coating the sample with a conductive material. Consequently, the SEM images showed the true surface characteristics of the nanoarray. These arrays were viewed at 20,000× (Fig. 3A) and 50,000× (Fig. 3B) magnifications.

Fluorescence imaging and analysis was conducted on a modified Olympus IX-81 inverted microscope [28] (Optical Analysis Co, Nashua, NH). The microscope contained a mercury light source, and excitation and emission filters (Chroma Technology, Rockingham, VT) were selected for visualization of Rhodamine B dye (excitation max at 550 nm; emission max at 605 nm) (Chroma HQ Set 31002). A Cooke Sensicam (Auburn Hills, MI) was used to image the fiber bundle and the fluorescence signals. The microscope stage had a suspended optical board in order to attach optical components. The fiber was held in a custom-built fiber holder using optical components from Newport Co. (Irvine, CA) and Linos Photonics (Milford, MA) perpendicular to the stage such that the etched fiber face pointed directly towards the objective lenses. The 700 nm nanoarray was viewed with a 50× (NA = 0.75) Olympus objective lens (Optical Analysis, Nashua, NH). The 300 nm nanoarray was viewed with an Olympus 60× water immersion lens (NA = 1.22) (Optical Analysis, Nashua, NH). For visualization, a water droplet was deposited onto a cover glass, and the 300 nm nanoarray was immersed in it to match the refractive indices of the sample and the objective lens.

3. Results and discussion

3.1. Characterization of nanoarrays by AFM and SEM

The imaging fiber bundles were etched using the difference in etching rates of the fiber core and cladding materials.

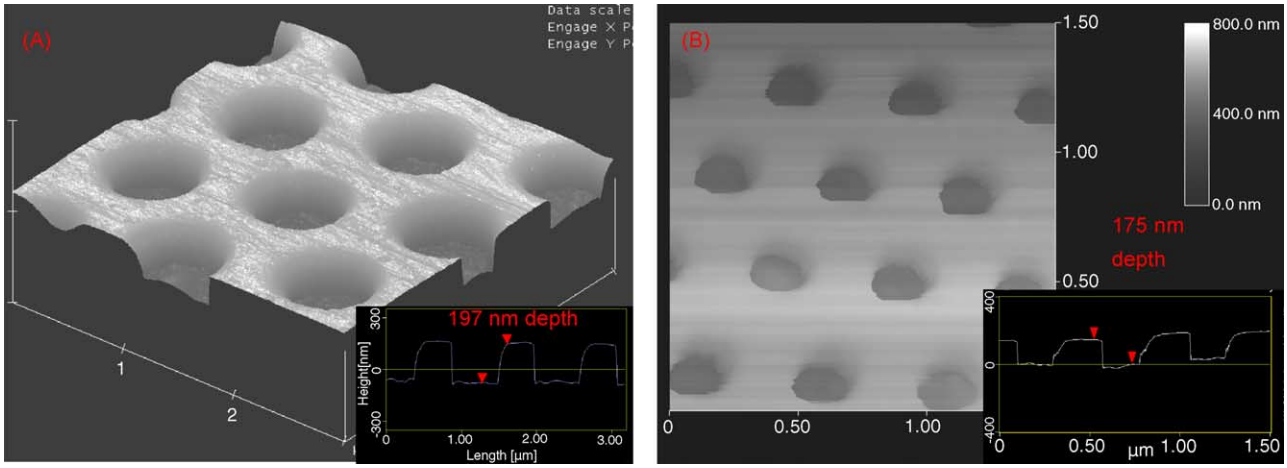

Fig. 1. Tapping-mode atomic force microscopy images of etched fiber bundles with nanometer sized cores. (A) 75 s etch of fiber bundle with 700 nm core sizes yields an etch depth of 197 nm. (B) 40 s etch of fiber bundle with 300 nm core sizes yields an etch depth of 175 nm.

A dilute HCl solution was used to etch the fibers and form the array of nanowells. Compared to other fabrication techniques [27,29,30], chemical etching provides a simple, rapid, and inexpensive method for creating a nanowell array.

The etch rate is dependent on the acid concentration and the fiber composition. At higher acid concentrations, the fiber bundle etched more quickly. Using several acid concentrations, it was determined that a 1 mM HCl concentration provided an etch rate that enabled good control over the etching depth. To determine the etch rate for each fiber bundle, polished bundles were immersed in 1 mM HCl for times ranging from 15 to 90 s, and the well depths were measured via scanning force microscopy (Fig. 1). The well depth was measured in the center of the fiber bundle in addition to three other regions on the fiber bundle face. The average well depth was calculated and plotted against the etching time to determine the etch rate of the fiber bundles (Fig. 2). By using SEM and AFM, the etch rate of the nanowells was calculated, and a desired well depth could be predicted.

To create sensor arrays, nanobeads were deposited into the etched nanoarrays. As described previously, beads were loaded onto the array using either of two methods: (1) depositing an aliquot of nanobead solution on the etched fiber bundle or; (2) mechanical force loading of dried beads into the nanowells. Both deposition techniques were successful with nanobeads, with approximately 50–60% of the wells filled upon the first loading using either method. While dry loading of the nanobead powder was effective, wet loading provided better control because the concentration of the nanobead stock solution could be adjusted.

Scanning electron microscopy images were taken of the nanowells to ensure that one nanobead was deposited into each nanowell using both wet and dry nanobead loading procedures. Fig. 3A shows a relatively low packing density of the 700 nm array prepared using an aliquot of low concentration bead solution. Fig. 3B shows a highly packed array fabricated with the dry loading method. These nanowells were etched deeper causing the nanobeads to be buried within the wells. The beads had a large polydispersity, accounting for the different relative heights of the nanobeads in the nanowells.

3.2. Optical characterization

Rhodamine B-dyed polystyrene and melamine beads were deposited onto the nanoarray in order to characterize their optical signals. Fig. 4 illustrates optically addressable nanoarrays with 700 nm beads (Fig. 4A) and with 300 nm beads (Fig. 4B). The images clearly show both occupied and empty wells. The spatial arrangement of the fluorescently labeled beads mimics the hexagonal packing structure of the etched fiber bundle, verifying array formation with the nanobeads.

In our standard microscale fiber bundle-based arrays, the individual beads are addressed by illuminating the proximal end of the fiber, and exciting fluorescence on the sensing

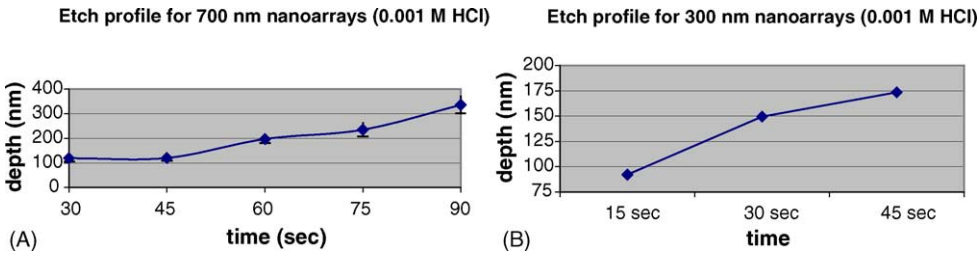

Fig. 2. Etch profiles for (A) 700 nm nanoarrays and (B) 300 nm nanoarrays.

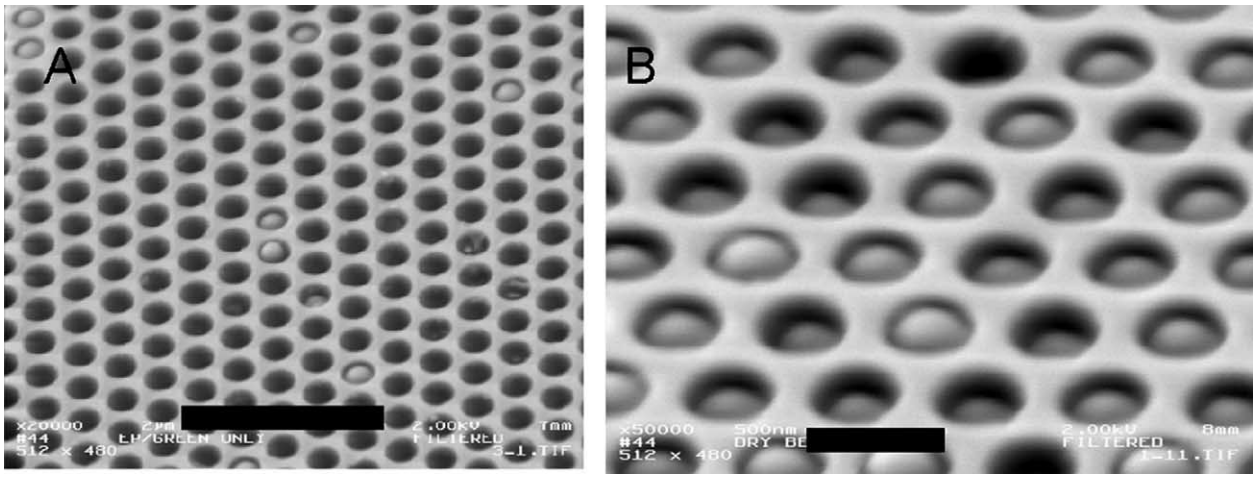

Fig. 3. Scanning electron microscopy images of (A) 700 nm nanofibers at 20,000× magnification and (B) 300 nm nanofibers at 50,000× magnification loaded with nanobeads.

beads at the distal face. These signals are transmitted back through the fiber to the objective lens and CCD camera for analysis [12,31]. In our present nanoarray, each fiber element is close to the diffraction limit of the light used to excite the fluorescent beads on the etched face of the fiber. As a result, light cannot be transmitted through these fibers. Instead, these beads must be addressed directly on the proximal face of the fiber.

The 700 nm nanoarray was viewed using a conventional 50× objective lens. The 300 nm nanospheres have dimensions close to the diffraction limit of light, making it necessary to use lenses with high numerical apertures in order to fully resolve the array. A water immersion objective lens was needed in order to adequately resolve the packing structure of the 300 nm nanoarray and view the individual nanobeads. The nanoarray was viewed through a water droplet in order to match the refractive index of the objective lens. Excitation (540 ± 13 nm) and emission filters (605 ± 23 nm) were used to measure the Rhodamine B intensities on the nanobeads.

The resolution limit of an optical system determines the degree to which a system can differentiate between two points. With higher resolving power, a smaller distance between two points can be distinguished. In standard far-field optics, the resolution limit is determined by the Abbè diffraction limit [32], which is approximately $\lambda/\{2(\mathrm{NA})\}$, where λ is the wavelength and NA is the numerical aperture of the lens. Given a fixed λ, greater resolving power can be achieved by increasing the NA. The minimum resolution for an optical microscope is accepted to be 0.25 μm [33].

An advantage of these nanoarrays is their ability to be resolved by conventional optical microscopy. As feature sizes become smaller, the signal intensities decrease and arrays become harder to optically resolve. Smaller features require the use of more sensitive detectors, such as avalanche photodiodes. In the arrays reported in this paper, signal amplification techniques are not required and the periodicity of the array fits within the minimum resolution limit of optical systems; therefore, a standard CCD camera can be used

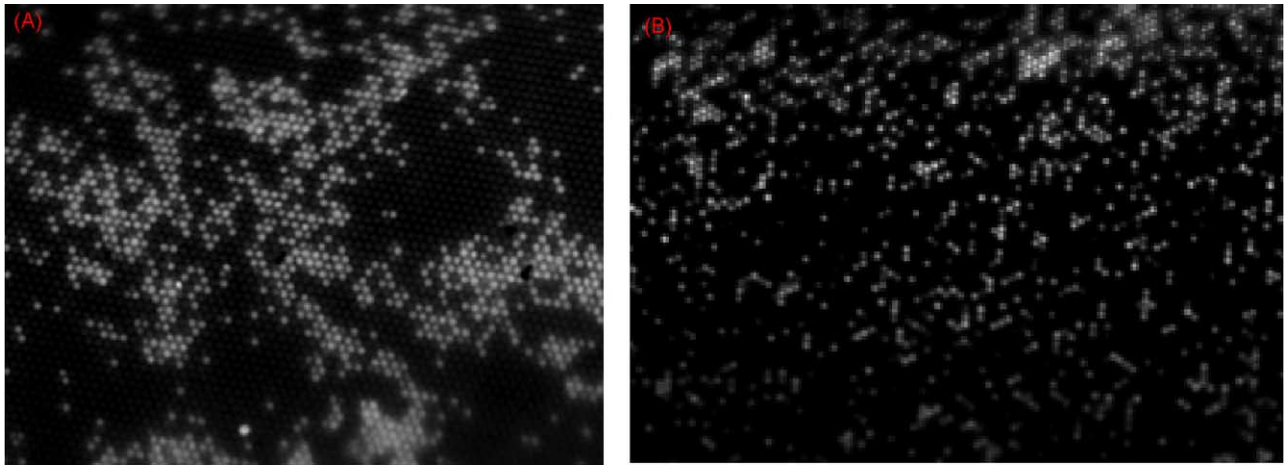

Fig. 4. Fluorescent images of arrays containing Rhodamine B-dyed nanospheres (A) 700 nm nanofiber array viewed with a 50× objective and (B) 300 nm nanofiber array viewed with a 60× water immersion objective.

to analyze the array elements. One nanoarray had 300 nm feature sizes with a 500 nm center-to-center distance, and the other nanoarray had 700 nm feature sizes with a 1 μm center-to-center distance. The center-to-center distance of 500 nm is twice the 250 nm resolution limit of optical systems, so that many array elements can be read in parallel. In addition, although the size of the particles is close to the diffraction limit of light (300 nm diameter particles at a $\lambda = 605$ nm emission), the beads were still resolved.

4. Conclusion

We have fabricated nanoarrays with 700 and 300 nm feature sizes using a simple two-step polishing and etching procedure to create nanowells. The nanowells were then loaded with fluorescently labeled nanospheres in order to characterize the arrays' optical properties. These nanoarrays have an ultra-dense packing structure such that a tremendous number of array elements can be read in parallel. These nanoarrays can be visualized and analyzed using conventional optical microscopy, using a simple, straightforward setup. For example, although the 300 nm nanospheres had dimensions close to the diffraction limit of light, they could be viewed using a water immersion lens with a high numerical aperture, which fully resolved the nanoarray. The arrays are ideal for high-throughput applications due to the large number of sensor elements, with up to 4.5×10^6 elements/mm^2. Applications, such as vapor detection and genomics analysis using these nanoarrays are the subject of our ongoing efforts.

Acknowledgements

We thank Schott Fiber Optics (Southbridge, MA) for providing us with the nanofiber arrays and for helpful discussions. This project was supported by DARPA (Defense Advanced Research Projects Agency) (2763-TU-ONR-0659).

References

[1] S. Venkatasubbarao, Trends Biotechnol. 22 (2004) 630.
[2] U. Nubel, P.M. Schmidt, E. Reiss, F. Bier, W. Beyer, D. Naumann, FEMS Microbiol. Lett. 240 (2004) 215.
[3] D.W. Nebert, E.S. Vesell, Eur. J. Pharmacol. 500 (2004) 267.
[4] K.K. Mantripragada, P.G. Buckley, T.D. de Stahl, J.P. Dumanski, Trends Genet. 20 (2004) 87.
[5] A. Bruckbauer, D.J. Zhou, D.J. Kang, Y.E. Korchev, C. Abell, D. Klenerman, J. Am. Chem. Soc. 126 (2004) 6508.
[6] J. Hyun, W.K. Lee, N. Nath, A. Chilkoti, S. Zauscher, J. Am. Chem. Soc. 126 (2004) 7330.
[7] L. Demers, G. della Cioppa, Genet. Eng. News 23 (2003) 36.
[8] M. Lynch, C. Mosher, J. Huff, S. Nettikadan, J. Johnson, E. Henderson, Proteomics 4 (2004) 1695.
[9] A. Hozumi, T. Saito, N. Shirahata, Y. Yokogawa, T. Kameyama, J. Vac. Sci. Technol. A 22 (2004) 1836.
[10] M.D. Yan, M.A. Bartlett, Nano Lett. 2 (2002) 275.
[11] T.A. Dickinson, J. White, J.S. Kauer, D.R. Walt, Nature 382 (1996) 697.
[12] J.A. Ferguson, F.J. Steemers, D.R. Walt, Anal. Chem. 72 (2000) 5618.
[13] T.A. Dickinson, K.L. Michael, J.S. Kauer, D.R. Walt, Anal. Chem. 71 (1999) 2192.
[14] S.E. Stitzel, D.R. Stein, D.R. Walt, J. Am. Chem. Soc. 125 (2003) 3684.
[15] K.J. Albert, D.R. Walt, Anal. Chem. 75 (2003) 4161.
[16] F.J. Steemers, J.A. Ferguson, D.R. Walt, Nat. Biotechnol. 18 (2000) 91.
[17] Y. Kuang, I. Biran, D.R. Walt, Anal. Chem. 76 (2004) 2902.
[18] J.R. Epstein, A.P.K. Leung, K.H. Lee, D.R. Walt, Biosens. Bioelectron. 18 (2003) 541.
[19] F. Szurdoki, K.L. Michael, D.R. Walt, Anal. Chem. 291 (2001) 219.
[20] Shuji Mononobe, Motoichi Ohtsu, J. Lightwave Technol. 14 (1996) 2231.
[21] S. Mononobe, M. Naya, T. Saiki, M. Ohtsu, Appl. Opt. 36 (1997) 1496.
[22] Y.-H. Liu, T.H. Dam, P. Pantano, Anal. Chim. Acta 419 (2000) 215.
[23] A. Sayah, C. Philipona, P. Lambelet, M. Pfeffer, F. Marquis-Weible, Ultramicroscopy 71 (1998) 59.
[24] W. Tan, Z.-Y. Shi, R. Kopelman, Anal. Chem. 64 (1992) 2985.
[25] W. Tan, Z.-Y. Shi, S. Smith, D. Birnbaum, R. Kopelman, Science 258 (1992) 778.
[26] P. Pantano, D.R. Walt, Chem. Mater. 8 (1996) 2832.
[27] S.P.A. Fodor, J.L. Read, M.C. Pirrung, L. Stryer, A.T. Lu, D. Solas, Science 251 (1991) 767.
[28] J.M. Tam, I. Biran, D.R. Walt, Appl. Phys. Lett. 84 (2004) 4289.
[29] A.P. Blanchard, R.J. Kaiser, L.E. Hood, Biosens. Bioelectron. 11 (1996) 687.
[30] M. Schena, D. Shalon, R.W. Davis, P.O. Brown, Science 270 (1995) 467.
[31] K.J. Albert, D.R. Walt, D.S. Gill, T.C. Pearce, Anal. Chem. 73 (2001) 2501.
[32] E. Abbe, Arch. Mikrosk. Anat. 9 (1873) 413.
[33] M. Abramowitz, Optics: A Primer, Olympus America, Lake Success, NY, 1994.